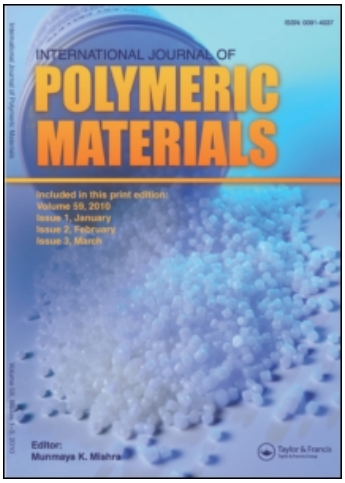

International Journal of Polymeric Materials
Publication details, including instructions for authors and subscription information:
http://www.informaworld.com/smpp/title~content=t713647664

Thermal and chemical effects of nucleating agents on α, β, γ-polymorphism of isotactic polypropylene

H. Dweik[a]; A. Al-Jabareen[a]; G. Marom[b]; E. Assouline[b]
[a] Department of Chemistry and Technology, AL-Quds University, Jerusalem, Palestine [b] Casali Institute of Applied Chemistry, The Hebrew University of Jerusalem, Jerusalem, Israel

Online publication date: 27 October 2010

To cite this Article Dweik, H. , Al-Jabareen, A. , Marom, G. and Assouline, E.(2003) 'Thermal and chemical effects of nucleating agents on α, β, γ-polymorphism of isotactic polypropylene', International Journal of Polymeric Materials, 52: 7, 655 — 672
To link to this Article: DOI: 10.1080/00914030304900
URL: http://dx.doi.org/10.1080/00914030304900

International Journal of Polymeric Materials, 52:655–672, 2003

ISSN: 0091-4037 print/1543-5253 online
DOI: 10.1080/00914030390198607

Taylor & Francis
Taylor & Francis Group

THERMAL AND CHEMICAL EFFECTS OF NUCLEATING AGENTS ON α, β, γ-POLYMORPHISM OF ISOTACTIC POLYPROPYLENE

H. Dweik
A. Al-Jabareen
Department of Chemistry and Technology,
AL-Quds University, Jerusalem, Palestine

G. Marom
E. Assouline
Casali Institute of Applied Chemistry,
The Hebrew University of Jerusalem,
Jerusalem, Israel

Isotactic polyprpylene (iPP) occurs in several crystalline forms, denoted as α (monoclinic), β (hexagonal), and γ (orthorhombic) phases. Hot-stage microscopy, differential scanning calorimetery, and wide-angle X-ray diffraction were used to investigate the influence of thermal treatment and nucleating agents on the morphology of iPP matrices. The tendency of glass fiber (GF) and Kevlar aramid fiber (KF) to induce transcrystallinity in different iPP matrices was evaluated. The α form was present in all iPP specimens treated by different nucleating agents at different crystallization temperatures (Tc). The β and γ forms (impure) were found only in iPP specimens that were treated with β-nucleating agent and γ- nucleating agent, respectively. Development of transcrystallization was found to depend on the type of fiber used, nucleating agents, and Tc. It was observed that the crystallinity content, obtained by applying different thermal treatments (slow cooling or quenching), gave rise to different morphologies of iPP matrices.

INTRODUCTION

Isotactic polyproplyene (iPP) is capable of crystallizing in four crystalline forms [1]. In melt-crystallized material, the dominant form is

Received 18 January 2003; in final form 21 January 2003.
Address correspondence to H. Dweik, Department of Chemistry and Technology, Al-Quds University, Jerusalem, Palestine. E-mail: hdweik@planet.edu

the α (monoclinic) form [2, 3]. The β (hexagonal) [4] form generally occurs at levels of only a few percent unless certain nucleating agents are present [2, 5], or if the crystallization has occurred in a temperature gradient [6, 7], or in the presence of shearing forces [7, 8]. The γ (orthorhombic) [9, 10] form occurs also at low levels, which is only observed in low molecular weight samples [11], or in high molecular weight samples in the presence of special nucleating agents [12], or in the samples that have been crystallized at high pressures [10, 13]. The fourth form is the smectic phase [1] that can be obtained if iPP is quenched from the melt at low temperature [2, 14] or when the crystallization occurs at high cooling rate [15].

In fiber-reinforced semicrystalline polymer composites, the mechanical performance is usually enhanced. This is due to the presence of the fibers, the polymer matrix, and the high interfacial adhesion between the two systems. The good adhesion is due to the presence of very regular columnar crystalline layer around the fiber, called transcrystallinity (tc) layer. The morphology and the mechanical propreties of the tc layer are different from those of spherulites, which normally form without the existence of fibers. The occurrence of tc layer enhances the longitudinal ultimate strength and modulus [16–18] and depends on many parameters such as crystallization temperature (Tc) [19, 20], types of fiber [19, 21–23], interfacial stress [2, 19, 24], and nucleating agents [24–26].

The objectives of this study are to see the effects of both nucleating agents and thermal treatments on the morphology of iPP. Moreover, microcomposites of treated glass fiber and Kevlar 149 fiber in different iPP matrices were examined.

EXPERIMENTAL

Sample Preparation

Aramid Kevlar 149 (KF) fibers were obtained from Du Pont, and glass fibers (GF) from Vetrotex International. Both had diameters of 12 and 14 μm, respectively. Glass fibers do not induce transcrystallization except under shear stresses. Thus they were coated with red quinadrone pigment, a β-nucleating agent. The pigment was dissolved in dimethylformamide (at about 0.1% in weight). The fiber was steeped in this solution for 4 h and then dried overnight in an oven at 160°C. The matrices were commercial iPP, provided by ExxonMobil. Their characteristics are reported in Table 1.

The iPP films (thickness in the range 70–130 μm) were prepared in a Carver press by pressing the polymer powder between two metal

TABLE 1 Molecular Characteristics, Designation, and Thermal Treatments of iPP Matrices

iPP matrix	Mw	Mn	Sample code	Thermal treatment	Remarks
MFR12	212500	43600	iPP1A	Air cooled	—
(iPP1)			iPP1Q	Quenched	
βtreated MFR12	212500	43600	iPP2A	Air cooled	β-nucleating
(iPP2)			iPP2Q	Quenched	agent
			iPP2I	124°C	
			iPP2II	130°C	
			iPP2III	135°C	
Achieve 3825	151000	75000	iPP3A	Air cooled	Metallocene-
(iPP3)			iPPP3Q	Quenched	based iPP
			iPP3I	124°C	
			iPP3II	130°C	
			iPP3III	135°C	
βtreated Achieve	151000	75000	iPP4I	124°C	β-nucleating
3825			iPP4II	130°C	agent
(iPP4)			iPP4III	135°C	

plates with minimal pressure. Pressing was performed at 190°C for 5 min, followed by quenching in ice water.

Crystalline iPP films were prepared at different crystallization temperatures (Tc) as follows: a small piece of iPP film (about 1 cm^2) was placed on a glass slide. A thin glass slide was placed above the sample to prevent the molten iPP from adhering to the upper plate of the hot-stage. A hot-stage (Mettler FP82) was used to heat the sample to 200°C, at heating rate of 20°C/min for 10 min to erase the previous thermal effects and then to decrease the temperature down to the chosen crystallization temperature.

Crystallization was carried out at different Tc's and nine types of samples were prepared. The designation of the different samples and their thermal treatments are given in Table 1.

The nonisothermal behavior of the different iPP samples was investigated for two different thermal treatments. The samples were either air-cooled (allowing the sample to cool between open press plates until the temperature reached 100°C, then the sample was removed to cool at room temperature) or they were quenched in ice water. Six types of samples were prepared as shown in Table 1.

Thermal Analysis

The apparent melting temperature (Tm) and degree of crystallinity (Xc) of the iPP samples were determined by using a Mettler TA-4000

differential scanning calorimeter (DSC). It is equipped with a control and programming unit operating under nitrogen atmosphere, using an empty capsule as reference. Samples (from 2.8 to 11.45 mg) were heated from 25 to 220°C at a heating rate of 10°C/min at a flow rate of 50 ml/min. The values of Tm and the apparent enthalpy (ΔH*) were obtained from the maxima and the area of the melting peaks, respectively. The degree of crystallinity of iPP samples was calculated from Equation (1):

$$Xc = \Delta H^{*}/\Delta H^{\circ} \tag{1}$$

where ΔH° is the heat of fusion per gram of 100% crystalline iPP taken as 207.1 J/g for α-iPP [2, 27], 193.0 J/g for β-iPP [2], and 144.8 J/g for γ-iPP [13,28].

Hot Stage Optical Microscopy

A Nikon optical microscope equipped with cross polarizers allows one to watch the inner cell of the Mettler FP82 hot stage crystallization unit. The microscope is connected to a Sony video camera and to a picture printer.

Under isothermal conditions, the crystallization temperature ranged from 110 to 145°C for KF/iPP2, 139 to 149°C for GF/iPP2, 111 to 133°C for KF/iPP3, 115 to 140°C for GF/iPP3, 116 to 140°C for KF/iPP4 and GF/iPP4.

WAXD Measurements

Wide-angle X-ray diffraction (WAXD) patterns were recorded at room temperature using a PW/710-based diffractometer with a Geiger counter, connected to a computer. Th Cu Kα radiation was Ni-filtered ($\lambda = 0.154$ nm). The diffraction scans were collected over a period from 1–2 h in the range 0–60°.

The amount of β-modification (X_β) was calculated using Equation (2) [2]

$$X_\beta = h_{\beta 1}/h_{\beta 1} + (h_{\alpha 1} + h_{\alpha 2} + h_{\alpha 3}) \tag{2}$$

where $h_{\alpha 1}$, $h_{\alpha 2}$, and $h_{\alpha 3}$ are intensities of α-modification peaks corresponding to angles $2\theta = 14.2^{\circ}$, 17.0°, and 18.8°, respectively, and $h_{\beta 1}$ is the intensity of β-modification peak corresponding to angle $2\theta = 16.2^{\circ}$.

The amount of the γ-modification (X_γ) was calculated using Equation (3) [29]

$$X_\gamma = h_\gamma/(h_\gamma + h_\alpha) \tag{3}$$

where (h_α) is intensive of α-modification peak corresponding to angle $2\theta = 18.8^\circ$, and (h_γ) is the intensity of γ-modification peak corresponding to angle $2\theta = 20.2^\circ$.

RESULTS AND DISCUSSION

Characterization of the Matrices

The effect of the thermal treatment and of the presence of β-nucleating agent on the crystalline composition of iPP matrices, compositions which are described in Table 1, was investigated. Neat α-iPP, that was previously investigated [24], served as the reference.

Isothermal Crystallization

Alpha-Beta Mixtures. The amount of β phase in sample of type iPP2 was investigated as a function of crystallization temperature. The melting peaks displayed in the DSC measurements (Figure 1) show that at Tc = 124.0°C, two melting endotherms corresponding to β (Tm = 151.0°C) and α (Tm = 168.0°C) phases can be observed. The area under the β peak is larger than the one under the α peak. At Tc = 130.0°C, there is one large peak for β phase at about 154.0°C accompanied by an endothermic shoulder for α phase at about 165.0°C. At Tc = 135.0°C, only one large endotherm can be seen, where the α and β phases cannot be resolved. The melting points and the areas of the peaks as a function of crystallization temperature are summarized in Table 2. The melting point increased as the crystallization temperature is increased, in consistence with the Hoffman-Lorentzian law [2], Indeed, the poorer the crystallization conditions (low Tc), the less perfect is the polymer structure produced (lower degree of crystallinity, smaller size crystallites, lower melting point), implying a lower structural stability, which is reflected in the characteristic of the melting process [2]. Yet, it seems that when the crystallization temperature increased, the melting temperature of α phase decreased whereas the one of the β phase increases (see Figure 1).

X-ray diffraction data in Figure 2 show that the characteristic β-peak at $2\theta = 16.0^\circ$ appears very strongly at low Tc; its intensity decreased as Tc increased (Table 2). Conversely, the intensities of peaks characterizing the α phase increase as Tc increases.

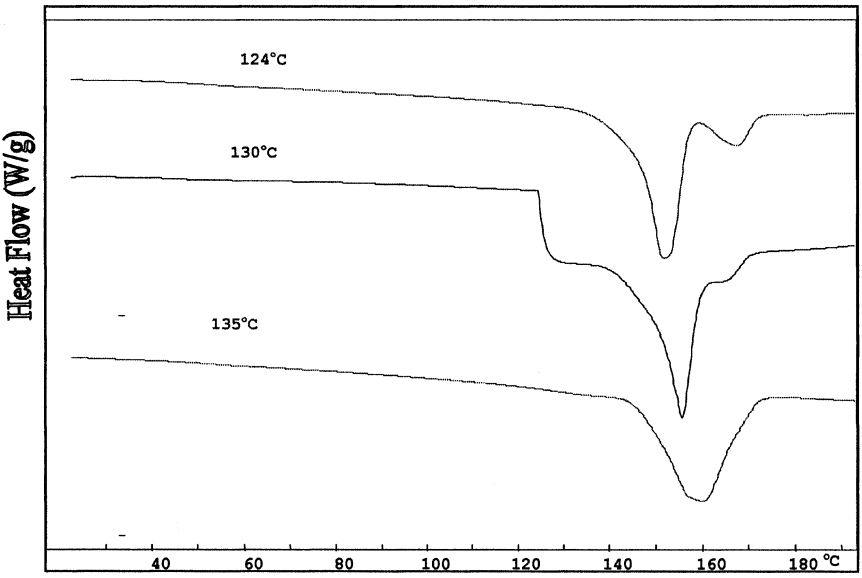

FIGURE 1 DSC curves of the iPP2 samples crystallized at different isothermal crystallization temperatures indicated.

TABLE 2 DSC and X-ray Characterization of iPP Samples at Different Tc

Sample code	Tc (°C)	Melting temperature (°C)[a]			Xc (%)[b]			Fraction $\beta/(\alpha + \beta)$[c]	Fraction $\gamma/(\alpha + \gamma)$[d]
		α	β	γ	α	β	γ	(–)	(–)
iPP2I	124	168	151	–	4.87	33.66	–	0.780	–
iPP2II	130	165	154	–	7.24	29.03	–	0.606	–
iPP2II	135	159	159	–	40.90	–	–	0.559	–
iPP3I	124	155	–	142	8.88	–	30.00	–	0.606
iPP3II	130	157	–	147	10.70	–	26.63	–	0.398
iPP3III	135	163	–	149	17.80	–	9.05	–	0.338
iPP4I	124	157	145	126	–	–	–	0.270	0.592
iPP4II	130	155	146	130	–	–	–	0.259	1.339
iPP4III	135	158	150	137	–	–	–	0.109	0.369

[a] Peak temperature of DSC endotherms during melting.
[b] Determined form DSC data according to Equation (1).
[c] Determined from WAXD data according to Equation (2).
[d] Determined from WAXD data according to Equation (3).

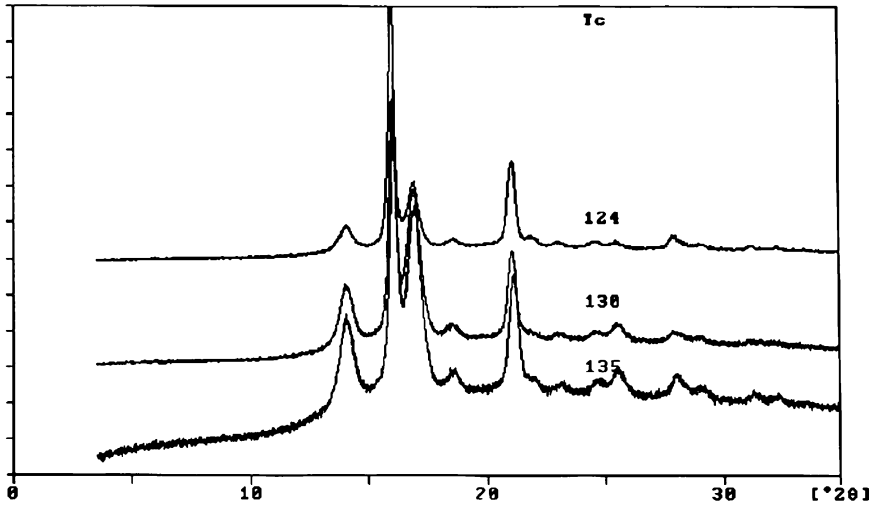

FIGURE 2 WAXD patterns of the iPP2 samples crystallized at different isothermal crystallization temperatures indicated.

Both measurements emphasize that the degree of crystallinity (Xc) decreased for the β phase as the temperature increased due to the lower melting point of β phase and to its presence in low amount. On the other hand, Xc increased for the α phase as the temperature increased due to the increase of crystallization temperature and its presence in larger amount (see Table 2).

Alpha-Gamma Mixtures. The effect of the crystallization temperature on the iPP3 samples is now investigated. At the three considered samples (124, 130, and 135°C), two melting peaks can be seen in Figure 3, one at (142, 147, and 149°C), probably corresponding to the γ phase, and one at (155, 157, and 163 °C) corresponding to the α phase. The peaks are better resolved as the crystallization temperature is higher, as seen in Figure 3. These DSC results are supported by X-ray data, shown in Figure 4. The α-peaks at $2\theta = 14.0^\circ$, 17.0°, 18.8°, and 25.8° appear very stongly at higher Tc (135°C) compared with low Tc. The γ-peak at $2\theta = 20.2^\circ$ appears very strongly at lower crystallization temperature.

The degree of crystallinity (Xc) is increased for the α phase as the temperature is increased due to its increased amount. On the other hand, Xc decreased for the γ phase as the temperature increased due to the lower melting point of γ phase and to its decreases amount as shown in Table 2.

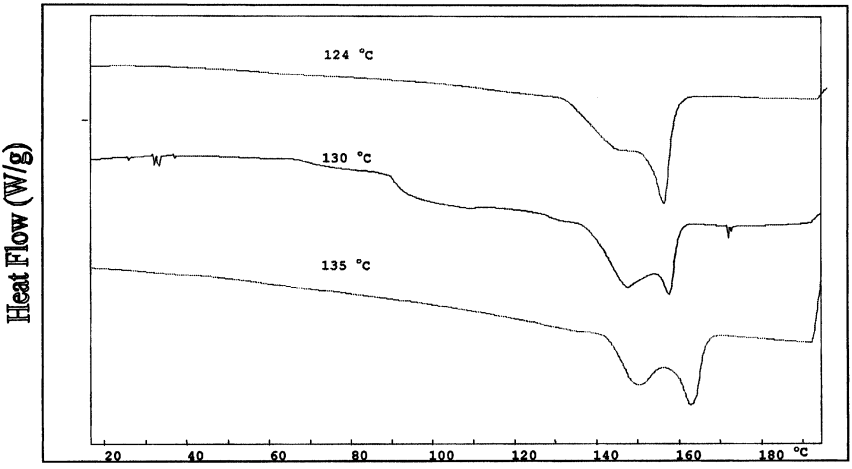

FIGURE 3 DSC curves of the iPP3 samples crystallized at different isothermal crystallization temperatures indicated.

It is concluded from Figure 3 and Table 2 that when the crystallization temperature increased the melting temperatures of α and γ phases increase. This can be explained by the fact that increasing the Tc leads to more perfect polymer structure (higher degree of crystallinity, larger size crystallites, higher melting point), suggesting a

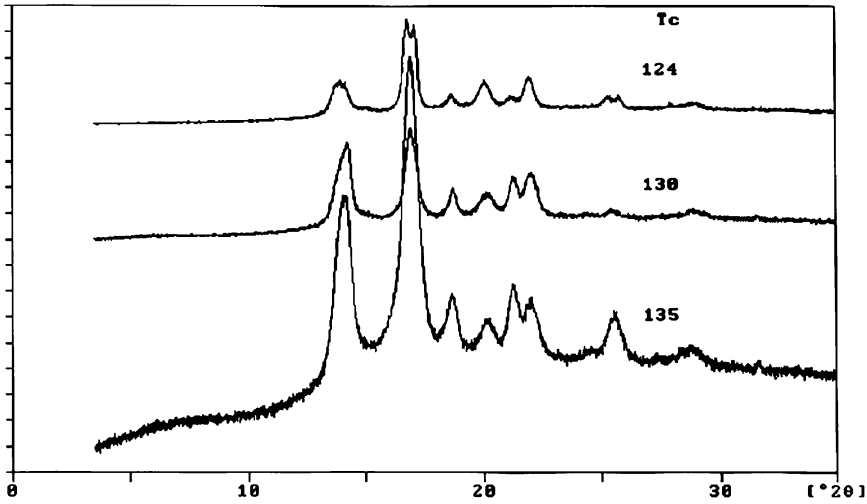

FIGURE 4 WAXD patterns of iPP3 samples crystallized at different isothermal crystallization temperatures indicated.

higher structural stability [2]. On the other hand, the amount of γ-modification (X_γ) that can be calculated using Equation (3) [29] decreased as the temperature increased due to the lower melting temperature of γ compared with α phase, as shown in Figure 3.

Alpha-Beta-Gamma Mixtures. The effect of crystallization temperature on the polymorphism of iPP4 samples was investigated. A mixture of the three polymorphs is expected.

From the DSC results shown in Figure 5, there are three melting endotherms for samples crystallized at Tc = 124°C. The first peak is for melting of γ phase (Tm = 126.0°C) and the others for β (Tm = 145.0°C) and α (Tm = 157.0°C) phases, respectively. At Tc = 130°C, there are three peaks. The first one is a shoulder for the melting of γ phase (Tm = 130.0°C), then there are two large peaks for β(Tm = 146.0°C) and α (Tm = 155.0°C), phases, respectively, which are separated by an exotherm. The third sample, which was crystallized at 135°C, also shows three peaks for γ (Tm = 137.0°C), β (Tm = 150.0°C) and α (Tm = 158.0°C) phases, respectively, which is an example of the unique crystalline polymorphism of iPP.

X-ray data in Figure 6 supported these results. The α-peaks at $2\theta = 14.0°$, 17.0°, 18.8° increased as the crystallization temperature

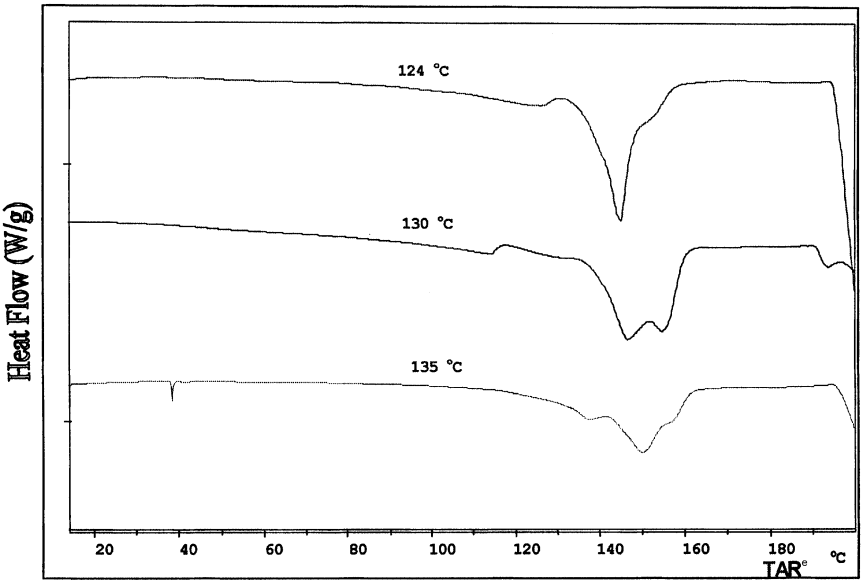

FIGURE 5 DSC melting curves of the iPP4 samples crystallized at different isothermal crystallization temperatures indicated.

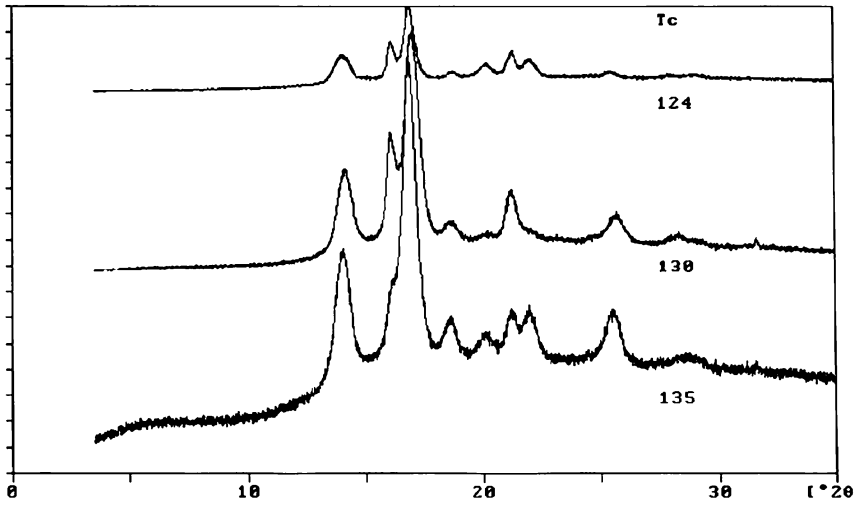

FIGURE 6 WAXD patterns of iPP4 samples crystallized at different isothermal crystallization temperatures indicated.

increased. On the other hand, the β-peak at $2\theta = 16.0^\circ$ appears only very weak at Tc = 135°C. Decreasing crystallization temperatures promote the formation of the β phase as for Tc = 130°C and 124°C. The γ-peak at $2\theta = 20.2^\circ$ appears in all samples that crystallized at different crystallization temperatures.

As the temperature increased, the melting temperatures of both β and γ phases increased. This can be explained by the fact that the increase in Tc leads to more perfect polymer structure (higher degree of crystallinity, larger size crystallites, higher melting point), implying a higher structural stability [2]. On the other hand, the melting temperature of the α phase is decreased at Tc 130°C but it increased at Tc 135°C as expected. For the fractions of β or γ phases of the used samples, in general, as the temperature is increased the amounts of these phases decrease, as shown in Table 2.

Nonisothermal Crystallization

Pure Alpha Matrices. The effect of thermal treatments on the melting and crystallization behavior of α phase was investigated.

The iPP1A and iPP1Q samples (Table 1) were characterized by DSC as shown in Figure 7. These samples contain only α phase despite the fact that sample iPP1Q shows two melting endotherms, one small at 160°C and another large peak at 173°C. The two endotherms occur as a result of the melting of the originally formed α crystals, and of the recrystallized α' crystals. This behavior confirmed the occurrence of

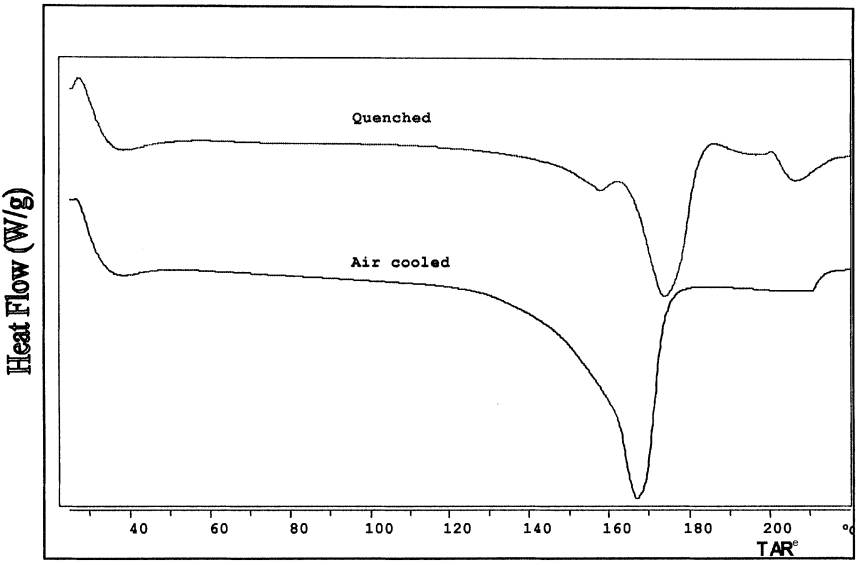

FIGURE 7 DSC melting curves of the iPP1 samples crystallized at different thermal treatments indicated.

partial recrystallization ($\alpha\alpha'$-recrystallization), causing an increase in the peak temperature of quenched sample (173.0°C) when compared with that of the air-cooled sample (165.0°C). Thus, under quenched conditions, the crystallization of α-iPP makes samples with a strongly expressed tendency to recrystallization caused by high structural instability as compared with samples under isothermal conditions.

TABLE 3 Characterization of Quenched and Air-cooled iPP Samples

Sample code	Melting temperature (°C)[a]					Xc (%)[b]		
	α	α'	β	β'	γ	α	β	Fraction $\gamma/(\alpha+\gamma)$[c] (–)
iPP1Q	160	173	–	–	–	25.6	–	–
iPP1A	165	–	–	–	–	54.2	–	–
iPP2Q	172	–	144	150	–	29.2	6.7	–
iPP2A	167	–	154	–	–	14.1	31.08	–
iPP3Q	154	–	–	–	–	–	–	0.917
iPP3A	160	–	–	–	142	–	–	0.827

[a] Peak temperature of DSC endotherms during melting.
[b] Determined form DSC data according to Equation (1).
[c] Determined from WAXD data according to Equation (3).

Furthermore, it is clear that the Xc for air-cooled sample is higher than that of quenched samples (see Table 3).

Alpha-Beta Mixtures. The effect of air-cooled and ice-quenched treatments on the morphology of iPP2 samples was investigated and the corresponding characteristics are shown in Table 3.

Figure 8 shows that iPP2A and iPP2Q samples exhibit two peaks in the air-cooled sample and three melting endotherms in the quenched samples. The two peaks occurring in the DSC experiments for iPP2A sample are caused by melting of the β phase at (154.0°C) and α phase at (167.0°C). In the case of iPP2Q samples, three peaks are observed, two small endotherms at 144°C and 150°C, separated by an exotherm. This indicates the process of melting of β and partly recrystallizing as β'($\beta\beta'$-recrystallization). The two endothermic and one exothermic peak occur below (155.0°C). In the melting process, a $\beta\beta'$-recrystallization takes place (i.e., without transition in the crystalline form), resulting in a duplication of the melting peak of β-phase. This is in accordance with the results by Varga [2,7]. The third peak (at 172.0°C) is due to the melting of the α phase. This recrystallization process or peak duplication causes, an increase in the peak temperature of the quenched sample compared with the air-cooled one. The value of Xc for β phase in the air-cooled samples is higher than that of the quenched sample as expected, but it is lower for air-cooled samples of the α-phase compared with the quenched one. This may be attributed to the low amount of α phase itself (see Table 3).

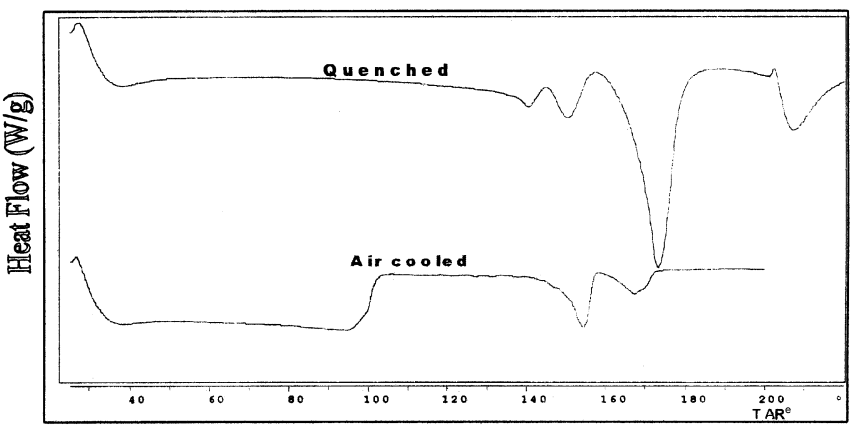

FIGURE 8 DSC melting curves of the iPP2 samples crystallized at different thermal treatments indicated.

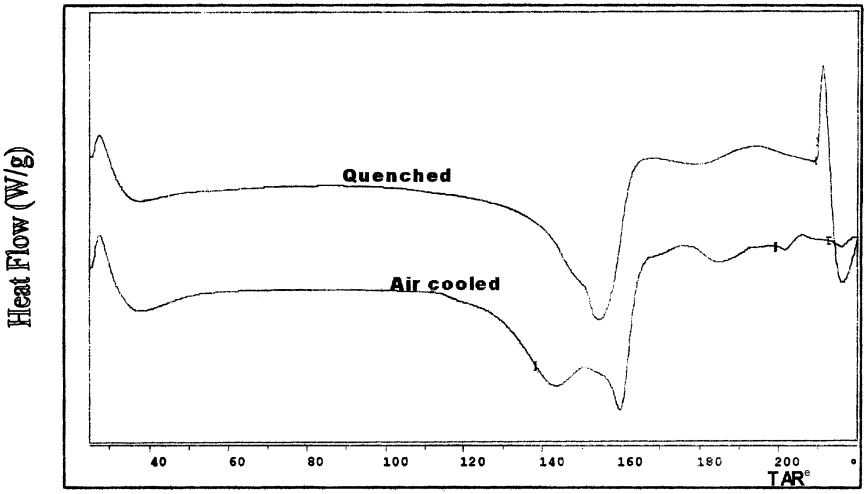

FIGURE 9 DSC melting curves of the iPP3 samples crystallized at different thermal treatments indicated.

Alpha-Gamma Mixtures. Figure 9 shows the DSC curves for iPP3Q sample and iPP3A. At temperatures around 154.0°C a peak appears for iPP3Q sample. This peak is due to the melting of α phase accompanied by an endothermic shoulder at about 147.0°C. This shoulder may be due to the melting of traces of γ phase. However, iPP3A shows two peaks at temperatures 142.0°C and 160.0°C that occur as a result of melting of the γ and α phases, respectively.

Comparing the melting temperatures of both quenched and air-cooled iPP3 samples, it can be seen that the melting temperature of the α-phase for the air-cooled sample is higher than the quenched sample. This may be due to the slow crystallization rate. We could not observe a behavior similar to the β phase (see Figure 8) where melting and recrystallization processes were shown. It appears that the presence of nucleating agents (metallocene catalyst) enhanced the structural stability of the γ phase [2]. On the other hand, the amount of γ phase in the quenched samples was more than in the air-cooled samples; results are listed in Table 3.

3.2 Development of Transcrystalinity on Fibers

When a polymer crystallizes on a nucleating fiber, the crystalline lamellae may grow only in the radial direction, to form a cylindrical layer: the transcrystalline layer. In contrast, in the bulk, the crystals

TABLE 4 Influence of Thermal Treatment on Fibre IPP Matrices

iPP matrix	Fiber	Tc range°C	tc layer
βtreated MFR12	KF 149	110–145	No
(iPP2)	GF(treated)	139–149	Yes
Achieve 3825	KF 149	111–133	Yes
(iPP3)	GF(treated)	115–140	Yes
βtreated Achieve 3825	KF 149	116–140	No
(iPP4)	GF(treated)	116–140	No

can develop in three dimensions, to produce spherulites. There is a competition between crystallization at the fiber surface and in the bulk. Finally, the growth of tc layer is hindered by the impingement with spherulites [20,30].

Table 4 lists the composites in which transcrystallinity has been observed, as a function of the crystallization temperature.

Fibers/β-Treated MFR12 iPP Systems

Kevlar fibers do not induce tc layer in β-treated MFR12 iPP matrix. It can be seen that the KF has no effect on the morphology of the iPP since the polymer looks fully spherulitic. The composition of the β-treated MFR12 matrix was studied as a function of the crystallization temperature Tc. It seemed that α phase is dominant in the bulk in comparison with the other phases, especially at high Tc, due to their melting behaviors. Although KF is known to induce large α-tc layer, nucleation occurs mostly in the bulk rather than at the KF surface because of the huge number of nucleation sites provided by the nucleating agent in the bulk. This prevents the formation of a tc layer around the fiber.

In contrast, a tc layer was observed on GF(treated) fiber. It is likely that the density of the nucleating agent at the fiber surface is greater than in the bulk. Crystal growth in this region developed when the crystallization temperature was above 140°C. Below Tc = 139°C, no tc layer was observed, unless it may have been indistinguishable from the spherulites in the bulk, due to fast formation of crystals in the bulk. A typical α-tc layer developed on treated-GF in a β-treated MFR12 iPP matrix as observed from its melting behavior.

Fibers/Achieve 3825 iPP Systems

Treated GF can generate tc layer in Achieve 3825 iPP-based composites within the whole range of the investigated temperatures (115–140°C). Figure 10 is a micrograph of GF(treated) that does induce transcrystallization. The tc region is seen as a white band of

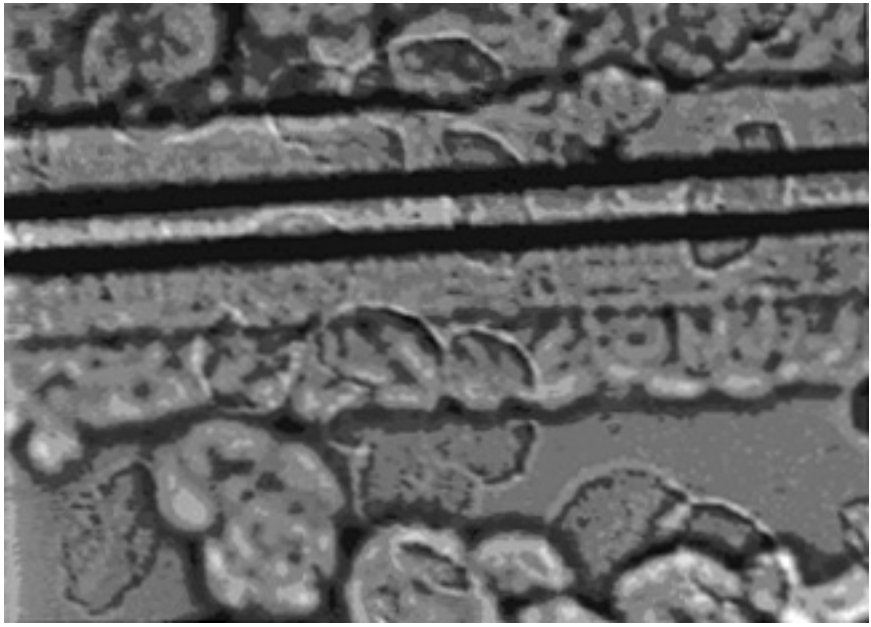

FIGURE 10 A photograph of α transcrystalline layer grown on GF.

densely packed lamella on both sides of the fiber. The uniform or parallel growth front of the tc layer reflects the uniform distribution of the nucleation sites on the surface of treated-GF. Since the melting point of the tc layer is about 165°C, it is concluded that the interface is fully α-tc. The α and γ form were found in the matrix after the thermal treatment. Though GF(treated) is known to induce β-tc layer, α-tc is still the dominant in the tc region also due to the matrix behavior.

Similarly, KF induces transcrystallinity in Achieve 3825 matrix, as seen in Figure 11, within a large Tc range (111–133°C). The helical shape of tc layer reflects helical defect along KF.

There is only one type of tc layer in this matrix, the α-tc layer. The melting behavior of α-tc layer was curified using the hot stage. It was shown previously that there were two crystalline forms of iPP3 (α and γ form) in this matrix in all the samples that were treated at different crystallization temperatures. Furthermore, KF exhibits α-tc layer. So it is expected that the tc-region be α or a mixture of two forms (α- and γ-tc). However, due to the large amount of α-form compared with γ form in the bulk, as shown in Table 2, especially at high Tc, it is expected that α-tc was the only form in the tc-region.

FIGURE 11 A photograph of α transcrystalline layer grown on KF.

Below Tc = 111°C, it was difficult to measure or investigate tc-layer in this matrix due to fast formation of bulk-spherulites around the KF. At high Tc (>133°C), the formation of tc-layer developed over a long period of time (1–2 days).

Fibers/β-Treated Achieve 3825 iPP Systems

No transcrystallinity was induced in β-treated Achieve 3825 matrix when both GF(treated) and KF were used. β-treated Achieve 3825 matrix has β- and γ-nucleating agents in addition to the original α-nuclei. That means that there are huge numbers of nuclei in the bulk or matrix to induce spherulites during isothermal crystallization, so when the KF- or even GF-based composites were prepared, there was no transcrystallization in both cases, indicating the strong competition to form spherulites due to the large number of nucleation sites in the matrix itself, and to form tc-layer around the fibers, causing, finally, the two systems (KF-iPP and GF-iPP), to fail to induce transcrystallization.

CONCLUSIONS

The effects of nucleating agents and thermal treatments on the morphology of iPP were investigated. α-phase in pure form was found in neat iPP specimens and in impure form was present in all other iPP specimens. Impure β and γ forms were present in nucleated specimens only, which reflects the ability of nucleating agents. A unique polymorphism (α, β, and γ form) was obtained by using β-nucleating agent and metallocene-based iPP. In general, as the crystallization temperature increased, the amount of β-iPP and γ-iPP decreased and the amount of α-iPP increased. Peak duplication phenomena appeared in quenched samples, which reflects the structural instability of the samples. The presence of metallocene-based iPP enhanced the structural stability of the specimens, so there is no recrystallization process in these quenched samples.

The tendency of KF 149 and treated-GF to nucleate the iPP during isothermal crystallization has been evaluated. Tc layer was more likely to occur in treated GF-iPP than in KF-iPP systems. This reflects the efficiency of nucleating agents either as coatings on the surface of the fibers or as nuclei in the bulk of the matrices.

REFERENCES

[1] Varga, J. (1992). *J. Mater. Sci.* **27**, 2557.
[2] Karger-Kocsis, J. (1995). *Polypropylene Structure, Blends and Composites,* 1st ed., (Chapman and Hall, London), Vol.1, Chaps. 3 and 4.
[3] Natta, G. and Corradini, P. (1960). *Nouvo Cimento Suppl.*, **15**, 40.
[4] Turner-Jones, A. and Cobbold, A. J. (1968). *Polym. Lett.,* **6**, 539.
[5] Varga, J., Mudra, I., and Ehrentein, G. W. (1999). *J. Therm. Anal. Cal.*, **56**, 1047.
[6] Lotz, B. (1998). *Polymer*, **39**, 4561.
[7] Varga, J. and Ehrensten, G. W. (1996). *Polymer*, **37**, 5959.
[8] Varga, J. and Karger-Kocsis, J. (1993). *Composites Sci. Tech.*, **48**, 191.
[9] Bruckner, S. and Meille, S. V. (1989). *Nature*, **340**, 455.
[10] Assouline, E., Fulchiron, R., Gerard, J. F., Wachetl, E., Wagner, H. D., and Marom, G. (1999). *J. Polym. Sci., Part B: Polym. Phys.*, **37**, 2534.
[11] Lotz, B., Graff, S., and Wittmann, J. C. (1986). *J. Polym. Sci., Part B: Polym. Phys.*, **24**, 2017.
[12] Thoman, R., Wang, C., Kressler, J., and Mulhaut, R. (1996). *Macromolecules*, **29**, 8425.
[13] Angelloz, C., Fulchiron, R., Douillard, A., Chabert, B., Fillit, R., Vautrin, A., and David, L. (2000). *Macromolecules*, **33**, 4138.
[14] Vleeshouwers, S. (1997). *Polymer*, **38**, 3213.
[15] Piccarolo, S. (1992). *J. Appl. Polymer. Sci.*, **46**, 625.
[16] Avella, M., Martuscelli, E., Sellitti, C., and Garagani, E. (1987). *J. Mater. Sci.*, **22**, 3185.

[17] Karger-Kocsis, J. (1995). *Polypropylene Structure, Blends and Composites*, 1st ed., (Chapman and Hall), London, Vol. 1, Chap. 10.
[18] Salehi-Mobarakeh, H., Ait-kadi, A., and Brisson, J. (1996). *J. Polym. Eng. Sci.*, **36**, 778.
[19] Thomason, J. L. and Van Rooyen, A. A. (1992). *J. Mater. Sci.*, **27**, 897–907.
[20] Wang, C. and Liu, C.-R. (1999). *Polymer*, **40**, 289.
[21] Thomason, J. L. and Van Rooyen, A. A. V. (1992). *J. Mater. Sci.*, **27**, 5–11.
[22] Wang, C. and Liu, C.-R. (1997). *Polymer*, **38**, 4715.
[23] Zafeiropoulos, N. E., Baillie, C. A., and Matthews, F. L. (2001). *Composites: Part A: Applied Science and Manufacturing*, **32**, 525.
[24] Assouline, E., Pohl, S., Fulchiron, R., Gerard, J. F., Lustiger, A., Wagner, H. D., and Marom, G. (2000). *Polymer*, **41**, 7843.
[25] Varga, J. and Karger-Kocsis, J. (1994). *J. Mater. Sci. Lett.*, **13**, 1069.
[26] Incordona, S., Migliaresi, C., Wanger, H. D., Gilbert, A. H., and Marom, G. (1993). *Composite Sci. Tech.*, **47**, 43.
[27] Bu, H. S., Cheng, S. Z. D., and Wunderlich, B. (1988). *Makromolekulare Chemie, Rapid Communications*, **9**, 76.
[28] Mezghani, K. and Phillips, P. J. (1998). *Polymer*, **39**, 3735.
[29] Turner Junes, A. (1971). *Polymer*, **12**, 787.
[30] Wang, C. and Hwang, L. M. (1996). *J. Polym. Sci., Part B: Polym. Phys.*, **34**, 47.